Computers and Concrete, *Vol. 17, No. 2 (2016) 201-214*
DOI: http://dx.doi.org/10.12989/cac.2016.17.2.201

Analytical study of failure damage to 270,000-kL LNG storage tank under blast loading

Sang Won Lee, Seung Jai Choi and Jang-Ho Jay Kim*

Department of Civil and Environmental Engineering, Yonsei University, 50 Yonsei-ro, Seodaemun-gu, Seoul 120-749, Republic of Korea

(Received September 30, 2015, Revised November 25, 2015, Accepted December 4, 2015)

Abstract. The outer tank of a liquefied natural gas (LNG) storage tank is a longitudinally and meridianally pre-stressed concrete (PSC) wall structure. Because of the current trend of constructing larger LNG storage tanks, the pre-stressing forces required to increase wall strength must be significantly increased. Because of the increase in tank sizes and pre-stressing forces, an extreme loading scenario such as a bomb blast or an airplane crash needs to be investigated. Therefore, in this study, the blast resistance performance of LNG storage tanks was analyzed by conducting a blast simulation to investigate the safety of larger LNG storage tanks. Test data validation for a blast simulation of reinforced concrete panels was performed using a specific FEM code, LS-DYNA, prior to a full-scale blast simulation of the outer tank of a 270,000-kL LNG storage tank. Another objective of this study was to evaluate the safety and serviceability of an LNG storage tank with respect to varying amounts of explosive charge. The results of this study can be used as basic data for the design and safety evaluation of PSC LNG storage tanks.

Keywords: LNG storage tank; blast analysis; LS-DYNA; protective design; pre-stressed concrete

1. Introduction

The use of liquefied natural gas (LNG) as an alternative energy source to petroleum is growing rapidly worldwide. Therefore, demand for its storage as well as better design and construction of larger LNG storage tanks is growing drastically, as well as demand for. An LNG storage tank comprises inner and outer tanks. The inner tank is in direct contact with extremely low-temperature LNG down to −162°C, thereby requiring the inner tank to be a temperature-resistant and leak-proof structure. However, the outer tank encases and protects the inner tank, acting as a barrier against external environmental factors and fatal accidental scenarios such as a bomb blast or an airplane crash. Therefore, it is important that the outer tank becomes an ultimate protective structure for stored LNG. Research on LNG storage tank design and analysis has been actively conducted globally. Jeon *et al*. (2003) investigated the design parameters for designing fully protective large-capacity LNG storage tanks with high efficiency in terms of construction cost and

*Corresponding author, Professor, E-mail: jjhkim@yonsei.ac.kr

http://www.techno-press.org/?journal=cac&subpage=8 ISSN: 1598-8198 (Print), 1598-818X (Online)

site utilization. They investigated critical factors in determining the shape of LNG storage tanks, including the structural dimensions and resistance capacities of the outer and inner tanks. Delome *et al*. (2005) conducted and discussed a numerical analysis of the sloshing loads of LNG for a 140,000-kL LNG inner tank in a marine environment using the smoothed particle hydrodynamics (SPH) method. Many other study results on LNG storage tank design and analysis have also been published. However, most of the analytical studies on LNG storage tanks were analyses of inner tanks considering the pressure exerted on the tanks due to the movement of LNG, whereas little research has been conducted on the response of pre-stressed concrete (PSC) outer tanks under extreme loading scenarios such as in a blast or impact conditions.

In terms of the research trends in blast load-related studies, Luccioni *et al*. (2004) determined the overall behavior of a reinforced concrete (RC) building subjected to blast pressure generated by a 400-kg charge. They used an analytical simulation and experimental verification to predict the collapse behavior. Chen *et al.* (2014) attempted to analyze a PSC beam under blast loading using a blast simulation method calibrated with the experimental data for RC structures subjected to a blast load. Their study results showed that PSC beams have a higher structural stiffness, load carrying capacity, and crack resistance than RC beams. Although many previous experimental and analytical studies on extreme loading have been conducted (Alam and Kim 2012, Kim *et al.* 2012, Heo and Kunnath 2013), research on the blast analysis of full-scale PSC structures such as LNG storage tanks has not been attempted until now. Therefore, in this study, a behavioral analysis of the PSC outer tank of an LNG storage tank under blast loading was conducted using a specific commercial FEM code, LS-DYNA. Because there are no available blast test data on PSC members, the blast simulation model was calibrated with the available blast test data for RC panel members (Yi *et al.* 2009). To check the accuracy of the finite element analysis results, hourglass energy values of the simulation results were verified. Once the calibration was completed, a full-scale blast simulation of a PSC LNG outer tank with a capacity of 270,000-kL was performed. Using a full-scale 270,000-kL LNG storage tank model, the safety of the tank under various blast charge pressures was evaluated.

2. Experiment overview

As stated in the Introduction, data from a blast-loaded RC panel test performed by Yi *et al.*

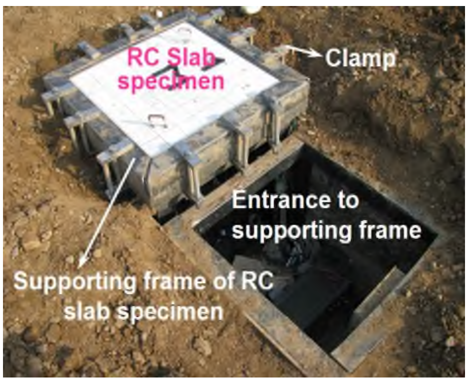

Fig. 1 Mesh grid of topographic model

Table 1 Material properties

Material Properties (Unit)		Value
Concrete	Compressive strength (MPa)	25.6
	Tensile strength (MPa)	2.20
	Young's modulus (GPa)	16.3
	Poisson's ratio	0.166
Reinforcing bar	Yield strength (MPa)	400
	Ultimate strength (MPa)	600
	Mass density (ton/m^3)	7.85
	Young's modulus (GPa)	200.0
	Poisson's ratio	0.3

(2009) was used to calibrate the simulation model. The blast experiment was conducted at the Defense Systems Test Center of the Agency for Defense Development in Korea. It was performed in two steps, namely, with preliminary and main blast tests. The preliminary test was conducted to estimate the appropriate amount of explosive charge to be used in the experiment to obtain the optimal measurements of applied pressure and deflections. From the preliminary test, it was determined that 15.88 kg (35 lbs) of ammonium nitrate/fuel oil (ANFO) with a 1.5-m standoff distance was the most suitable loading for the experiment. In the experiment, various types of RC panels were used as specimens. The panels were mounted at the ground surface level to minimize the blast pressure diffraction and interference. For the specimen mounting structure and data acquisition system, a steel truss chevron structure was constructed using SM-520, 7-mm-thick steel members, as shown in Fig. 1. Steel angles and clamps were used to fix the concrete specimens to the mounting structure. The dimensions of the specimens were 1,000 A? 1,000 A? 150 mm. The RC panels were reinforced with D10 rebar in an orthogonal arrangement at the top and bottom of each specimen. The D10 rebar had a yield and ultimate strength of 400 and 600 MPa, respectively. These were placed at 82-mm intervals in both directions. The properties of the materials used in the test are shown in Table 1.

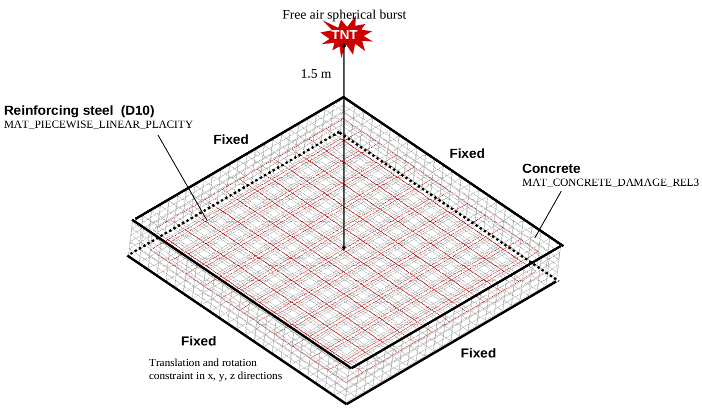

Fig. 2 Finite element slab models (reference)

3. Experimental verification based on analysis

Once detonated, a blast wave travels outward in a radial shape from the center of the explosive charge. This radial shape travels through the air as a sinusoidal wave with different arrival times and peak values of overpressure until it reaches the target surface. This causes the applied blast pressure distribution to be non-uniform, which results in a severe stress gradient on the structure. This gradient should be calculated using precise 3D finite element modeling of the test site and setup.

3.1 Boundary condition model

The concrete specimen and support frame structure in the blast experiments were fixed using angles and clamps. Therefore, the top and bottom of the reinforced panels were given a semi-fixed boundary condition, and the details of the modeling are shown in Fig. 2.

3.2 Material model

LS-DYNA offers a large number of material cards to be used as its constitutive models, including concrete material models such as *MAT_BRITTLE_DAMAGE (MAT_96), *MAT_ JOHNSON_HOLMQUIST_CONCRETE (MAT_111),*MAT_PSEUDO_TENSOR (MAT_16), *MAT_CSCM_CONCRETE (MAT_159), and *MAT_CONCRETE_DAMAGE_REL3 (MAT_ 72R3). In this study, *MAT_CONCRETE_DAMAGE_REL3 (MAT_72R3), which incorporates the characteristics of blast loading, was used. MAT_072R3 can incorporate a concrete strength development factor for the dynamic strain rate based on blast loading. The reliability of the material model in predicting the response of an RC structure subjected to blast loading was demonstrated by Jiang *et al*. (2012).

For rebar, *MAT_PIECEWISE_LINEAR_PLASTICITY (MAT_24) was used. This material model takes into account the isotropic and kinematic hardening plasticity. Moreover, it can define arbitrary stress versus strain and strain rate curves.

3.3 Blast load model

LS-DYNA provides the *LOAD_BLAST option, which simulates the blast loading applied to a structure. The accuracy of the changes in behavior of a structure due to blast loading measured using this option has been demonstrated in many studies (Qin and Pingan 2003, Yi *et al.* 2012, Li *et al.* 2006). In this study, the maximum pressure for reflective pressure waves when detonating 15.88 kg (35 lbs) of TNT at a distance of 1.5 m from the slab structure was estimated, and the load converted from the blast waves was applied non-homogenously to the entire surface of the concrete slab. The time history of the blast pressure and impulse are shown in Fig. 3.

3.4 Results discussion and comparison

To verify the accuracy of the analysis, separate measurements of the maximum deflection and residual displacement of the specimen were performed. In the performed experiments, the maximum deflection was obtained from a linear variable differential transformer (LVDT) placed at the center of the bottom surface of the concrete specimens. The deflection behavior and residual

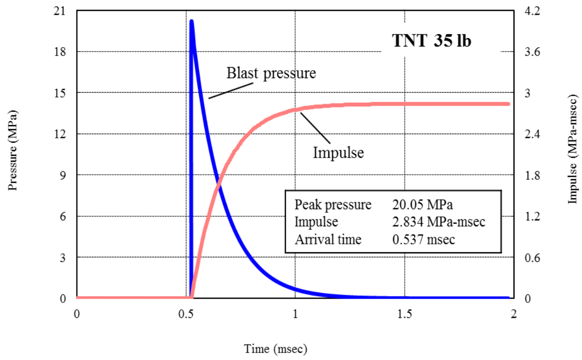

Fig. 3 Pressure-time history (reference)

Table 2 Comparison of experimental and analytical maximum displacement results

	Experiment	Analysis
Maximum displacement (mm)	24.40	27.01

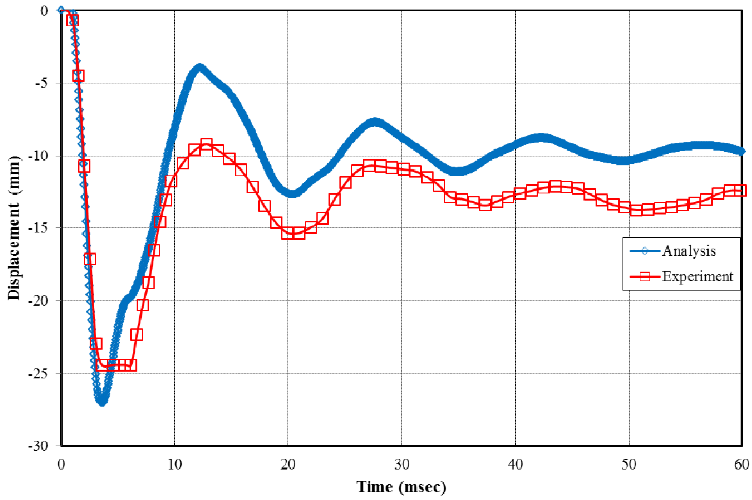

Fig. 4 Comparison of experimental and analytical displacement results

displacement were measured using LVDTs placed at various locations on the bottom surface of the specimens. A comparison of the test data and simulation results in Fig. 4 and Table 2 shows that the maximum deflection and residual displacement in the analytical results were within the allowable error range of the experimental results, suggesting their validity. Therefore, it was safe to assume that the simulation material and structural models used in the blast simulation of the RC panel could be used for the full-scale blast simulation of a PSC LNG storage tank.

3.5 Hourglass energy evaluation

Blast simulations were performed using reduced integration elements, and the results were

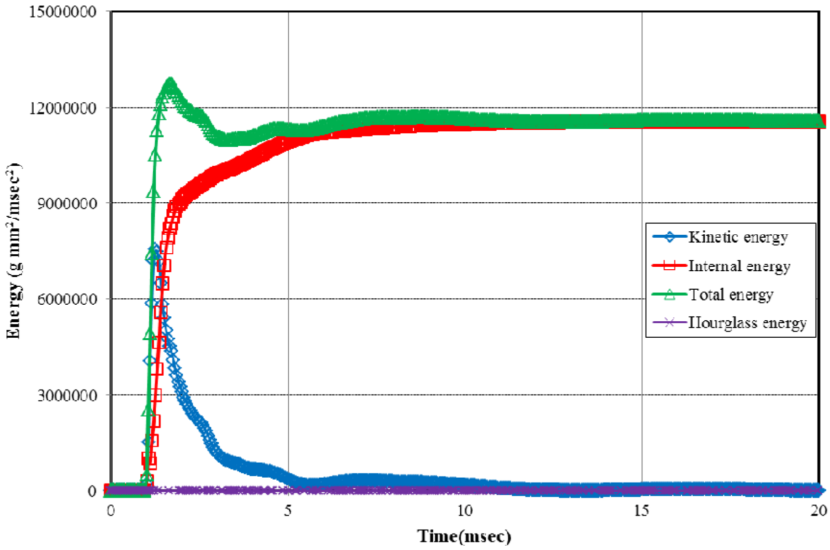

Fig. 5 Energy results from the analysis model

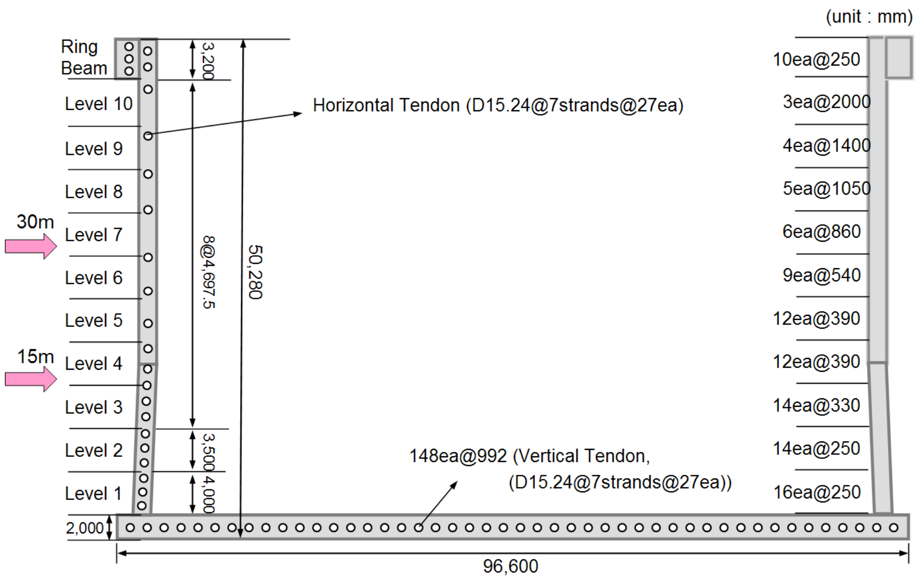

Fig. 6 Cross-section details of 270,000-kL LNG tank

compared with those obtained using fully integrated elements. The simulation results show that the stress levels obtained using reduced integration elements are less than those obtained using fully integrated elements. The hourglass energy results obtained from the blast simulation of an RC panel were checked and found to be less than 1.0%, as shown in Fig. 5. This value is much less than the acceptable limit of 10% of the internal energy of the process defined by the developers of LS-DYNA (Hallquist, 1993). The hourglass energy evaluation of the simulation results for a blast-loaded RC panel member confirmed that the simulation model is sufficiently accurate and can used to conduct the full-scale simulation of a 3D PSC LNG storage tank under blast loading.

4. Selection of LNG storage tank blast scenario

4.1 Selection of blast location

Based on the results of a previous study on blast loading, a charge location was selected, which would apply the most direct application of blast pressure onto the target structure without any type of environmental resistance or physical hindrance. Blast pressure was expected to create more significant stresses when applied at the lower region of the outer tank wall owing to a fixed support condition between the wall and support. To offset the different stress concentrations generated in the lower and upper regions of the wall, PS tendons were placed much more densely in the lower regions. The tendon and rebar arrangement used for the tank is shown in Fig. 6. Because of this biased arrangement over the height of the wall, the strength at the mid-height region of the wall is lower than that at support region. Therefore, the blast pressure targets for the full-scale simulations were selected at 30 m (mid-height region) and 15 m (support region) from ground level.

4.2 Blast analysis conditions

It was assumed that the blast would occur during normal operating conditions of the LNG storage tanks; accordingly, the outer tank was subjected to self-, pre-stressing, internal, and thermal loads during normal operating conditions. The internal and thermal pressures at these conditions were ignored since the internal tank and thermal cover layer would prevent the pressure and temperature of the LNG from reaching the outer wall.

5. Finite element model of outer tank

Although 2D modeling of the tank wall using shell elements would have yielded faster simulation results, 3D modeling was selected since there are problems associated with the idealized shell structure model, such as joint stiffness redundancy and discrepancies. Therefore, in this study, concrete cross-sections were modeled as solid elements using Hypermesh 11.0 and the actual material properties and nonlinearities of concrete, rebars, and PS tendons.

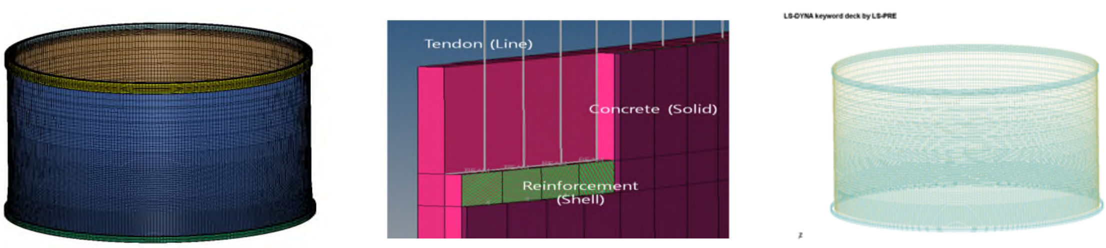

(a) Full modeling (b) Detail of modeling (c) PS tendon modeling

Fig. 7 Modeling of LNG tank

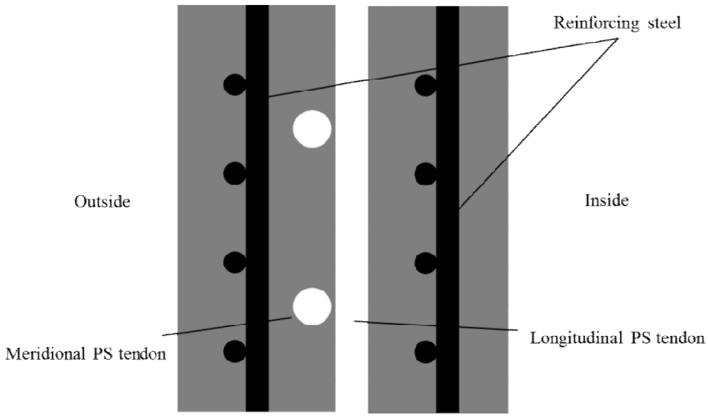

Fig. 8 Cross-section of LNG tank

Table 3 Material properties

	Material property (unit)	Value
Concrete	Mass density (ton/m^3)	2.4
	Compressive strength (MPa)	40
	Young's modulus (GPa)	31.75
	Poisson's ratio	0.2
Reinforcing steel	Mass density (ton/m^3)	7.85
	Yield strength (MPa)	400
	Young's modulus (GPa)	200.0
	Poisson's ratio	0.3
PS tendon	Mass density (ton/m^3)	7.85
	Young's modulus (GPa)	195.0
	Poisson's ratio	0.3
	Vertical PS force (MPa)	862.5
	Horizontal PS force (MPa)	1153

5.1 Geometric characteristics of outer tank

The structural details used in the blast analysis were the outer tank details of a 270,000-kL LNG storage tank with approximately 59.66 and 48.28 m in height from the base slab to the domed roof and ring beam, respectively. The internal radius of the outer tank wall was 46.2 m with a varying thickness of 0.75-1.2 m. Fig. 6 shows a cross-sectional view of the outer tank, and Fig. 7 shows the actual finite element model of the structure. The wall was a PSC structure, and its cross-sectional view is shown in Fig. 8. The layout of PS tendons and rebars varied depending on the location of the wall, and the modeling of the walls reflected the actual details of a 270,000-kL LNG tank currently being constructed in Korea.

5.2 Physical properties of LNG storage tank modeling elements

The physical properties of each element used in modeling the outer tank are shown in Table 3.

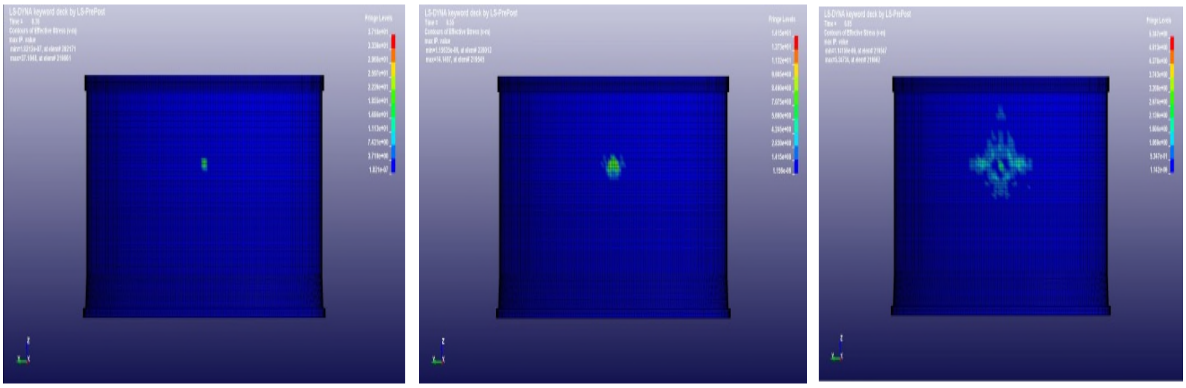

(a) 0.35 msec (b) 0.55 msec (c) 0.85 msec

Fig. 9 Von-Mises stress behavior

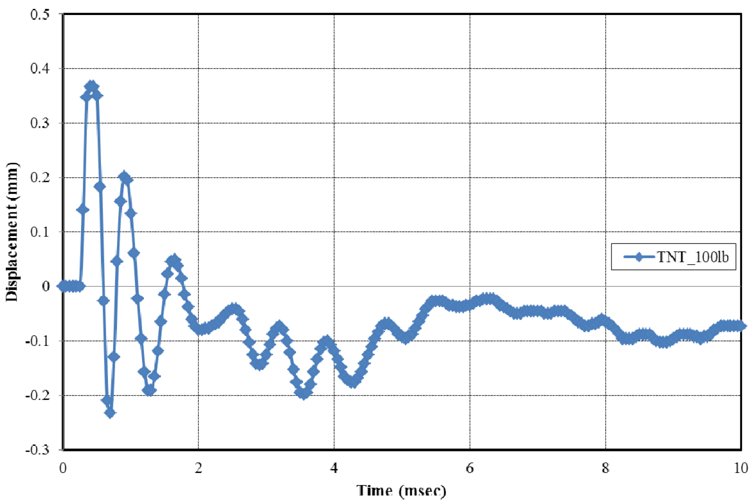

Fig. 10 Displacement-time history

The model used the same values for the material and structural properties as were used in the actual design.

5.3 Finite element model details

Detailed modeling of the rebar layout was deemed unnecessary since the purpose of the analysis was to determine the overall behavior of the structure rather than a localized one. Moreover, it would be nearly impossible to conduct a blast simulation using a structural model with individual rebars. Therefore, the rebars were idealized as a shell structure with the appropriate stiffness and strength, embedded in the solid concrete elements.

In the case of PS tendons, which are a critical parameter in the overall behavior of the structure under blast loading, they were actually modeled as truss elements. The PS tendons were embedded in the concrete elements with the exact spacing and sizes that reflected the design layout and specifications of those used in the LNG tank. Moreover, a PS force had to be given to the truss members as an initial force condition to reflect the actual pre-stressing force applied to the tendons. This was applied using the Initial_Stress_Beam option provided by LS-DYNA. It was assumed that when this option was used, the initial force condition applied to a truss element would be maintained until the end of the simulation with no PS force loss.

6. Blast analysis results for outer tank

6.1 Blast behavior of LNG storage tank based on amount of explosives

Fig. 9 shows the changes in effective strain generated in the outer tank wall when pressure from a 45.36-kg (100 lbs) TNT blast charge with a standoff distance of 1.0 m was applied to the section at 30 m from ground level (i.e., mid-height region). As shown in the figure, the time history of the blast and wall behavior was instantaneous. It was found that the detonation of this large blast capacity of TNT resulted in the instantaneous application of a large impulsive pressure on the wall. Fig. 10 shows the maximum displacement versus time history at the wall, where the maximum displacement occurred. The graph shows that a maximum displacement of 0.23 mm occurred at 0.35 msec, when the blast activation was at its maximum level, and that the post-blast changes decreased progressively as the impulse dissipated, leaving negligible residual deformation at the end.

Fig. 11 shows the changes in effective stress versus time history for the stress-concentrated location where the maximum displacement occurred. The maximum stress occurred at 0.35 msec, when the blast activation was at its maximum level. The maximum effective stress was 37.1 MPa owing to a rapid increase in stress when the blast loading was applied. The stress then rapidly dissipated as the blast stress dispersed to the area surrounding the localized initial stress location.

While designing a PSC LNG storage tank wall for extreme conditions such as external blast loading, safety of the structure can be ensured by increasing the concrete strength through the application of a material development factor of 1.3. However, it was deemed unnecessary to increase strength by applying such a factor for the simulation. Therefore, an actual concrete

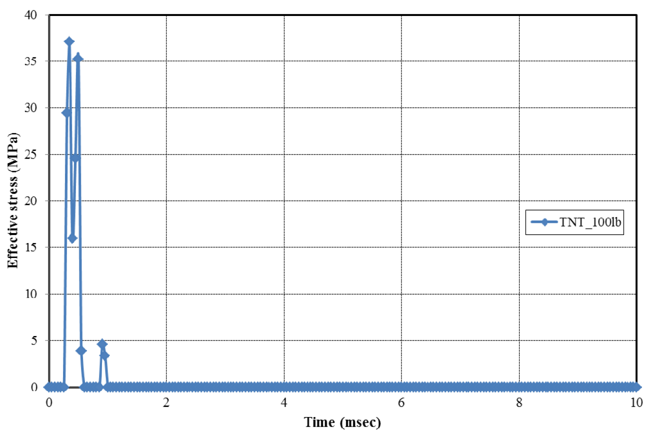

Fig. 11 Effective stress-time history

Table 4 Blast assessment

σ_{max} (MPa)	σ_a (MPa)	γ_f	σ'_a (MPa)	Blast assessment
37.1	40	1.207	48.28	$\sigma'_a > \sigma_{max}$ (No damage)

strength was used in the model because the simulation assumes that the concrete strength is fully satisfied. Therefore, a design compressive strength of 40 MPa was set as the compressive strength of concrete f_{ck} for the simulation. However, when determining failure of the PSC wall based on the blast-generated effective stress, the 1.3 development factor was multiplied by the concrete compressive strength to be conservative in determining failure of the material and structure. Therefore, failure of the concrete wall from blast loading was determined based on an allowable stress limit value equal to the design concrete strength multiplied by the development factor.

The present study employed the strength development factor used by Kim *et al*. (2007), which is capable of expressing high strain rates for impulsive pressures using a strength development factor that is based on experimental results. The maximum strain rate was 0.041 sec^{-1}, and the corresponding strength development factor was 1.207. Although the strength development effect should be implemented for rebars, PS tendons, and concrete in an ultimate load level state, only the factor for concrete was used in this study to consider the extreme loading effect. Therefore, the outer tank failure was assessed by comparing the maximum effective stress (σ_{max}) generated by the blast pressure and the allowable stress limit value (σ'_a) calculated as described in the previous sentence.

The final evaluation results are shown in Table 4. According to the results of the finite element analysis for an external blast loading scenario of 45.36 kg (100 lbs) of TNT, the maximum stress in the wall at the time of blast was 37.10 MPa, which is lower than the concrete allowable stress limit value of 48.28 MPa. This suggests that the wall would be safe against the 45.36 kg (100 lbs) of TNT detonation at a 1-m standoff distance. The localized initial stress concentration was dispersed to the area surrounding the localized initial stress location in the form of a shock wave and dissipated by the rebounding behavior of the wall. The small magnitude of the dispersed stresses indicates that the wall would not deform significantly from the stress dispersion effect.

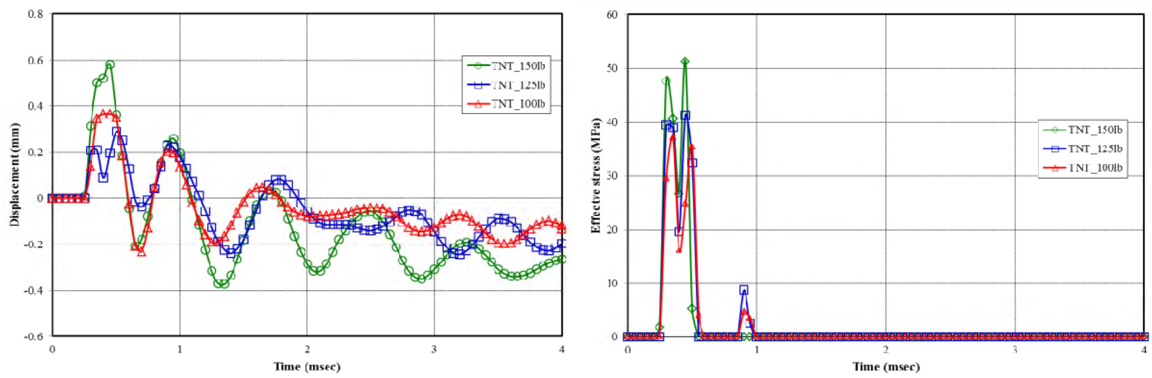

(a) Displacement (b) Effective stress

Fig. 12 Comparisons of displacement and effective stress

Table 5 Blast assessment

Amount of TNT	$\sigma_{\max}$ (MPa)	σ_a (MPa)	$\dot{\varepsilon}$	γ_f	σ'_a (MPa)	Blast assessment
45.36 kg (100 lbs)	37.1	40	0.041	1.207	48.28	$\sigma'_a > \sigma_{max}$
56.70 kg (125 lbs)	41.2	40	0.058	1.223	48.92	$\sigma'_a > \sigma_{max}$
68.04 kg (150 lbs)	51.2	40	0.131	1.263	50.52	$\sigma'_a < \sigma_{max}$

6.2 Determination of maximum amount of TNT explosives

The effect of the amount of TNT explosive charge on the tank was demonstrated by increasing the TNT amount from 56.70 kg (125 lbs) to 68.04 kg (150 lbs) at a standoff distance of 1 m at a blast pressure target location of 30 m from ground level. As expected, Fig. 12 shows that the maximum displacement and maximum effective stress increased as the amount of explosives increased.

Since an increase in the amount of explosive charge would lead to an increase in kinetic energy, the impulsive pressure applied to the wall would increase accordingly, resulting in a greater blast pressure effect on the structure. The results of the blast charge amount assessment graphs shown in Fig. 12 are summarized in Table 5. As shown in this table, the amounts of explosive charge up to 68.04 kg (150 lbs) can be considered safe against damage to the outer tank walls of the LNG storage tank. However, explosive charge amounts greater than 68.04 kg (150 lbs) can be considered catastrophic to the integrity of the outer tank wall. However, this assessment is only applicable to the 270,000-kL PSC LNG tank outer wall design used in the study, and a more detailed study must be performed to make a more general assessment applicable to outer wall structures of other PSC LNG tank.

7. Conclusions

In this study, the safety of the outer tank wall of a PSC LNG storage tank under the scenario of a blast charge detonation with a close proximity standoff distance was evaluated by conducting a blast simulation using a specific commercial finite element program (LS-DYNA). The following conclusions can be drawn from the study results

• The blast simulation of the outer tank with 45.36 kg (100 lbs) of TNT blast pressures applied at structurally vulnerable locations (support and mid-height regions) showed that the displaments were minimal compared to the stresses caused by blast loading.

• Using the blast damage criteria for the tank wall, a blast failure assessment of the PSC wall of a 270,000-kL LNG storage tank was performed.

• Owing to the instantaneous impulsive pressure applied to the wall from the explosive charge detonation of 45.36 kg (100 lbs) TNT at a close proximity of 1 m, the majority of the blast damage was from the initial instantaneous impulsive pressure applied to the wall.

• A full-scale simulation of the tank showed that the PSC outer wall of the 270,000-kL LNG storage tank can withstand up to 68.04 kg (150 lbs) of TNT charge exploding at a 1-m standoff distance.

Acknowledgments

This work was partially supported by the Nuclear Safety Research Program through the Korea Radiation Safety Foundation (KORSAFe) and financial resources granted by the Nuclear Safety and Security Commission (NSSC), Republic of Korea (No. 1403010). Also, this research was partially supported by a grant funded by Ministry of Land, Infrastructure and Transport of the Korean Government (14TBIP-CO74206-01).

References

Alam, M.I. and Kim, D. (2012), "Effect of constitutive material models on seismic response of two-story reinforced concrete frame", *Int. J. Concrete Struct. Mater.*, **6**(2), 101-110.

Baylot, J.T. and Bevins, T.L. (2007), "Effect of responding and failing structural components on the airblast pressures and loads on and inside of the structure", *Comput. Struct.*, **85**(11), 891-910.

Byun, K.J., Nam, J.W., Kim, H.J. and Kim, S.B. (2006), "Dynamic analysis of reinforced concrete wall under blast loading", *Proceeding of 2nd ACF International Conference*, Bali, November.

Chen, W. and Hao, H. (2012), "Numerical study of a new multi-arch double-layered blast-resistance door panel", *Int. J. Impact Eng.*, **43**, 16-28.

Chen, W., Hao, H. and Chen, S. (2015), "Numerical analysis of prestressed reinforced concrete beam subjected to blast loading", *Mater. Des.*, **65**, 662-674.

Chin, L.S. (2007), "Finite element modeling of hybrid-fiber ECC targets subjected to impact and blast", Ph.D. Dissertation, National University of Singapore, Singapore.

Dancygier, A.N. and Yankelevsky, D.Z. (1996), "High strength concrete response to hard projectile impact", *Int. J. Impact Eng.*, **18**(6), 583-599.

Delorme, L., Iglesias, A.S. and Perez, S.A. (2005), "Sloshing loads simulation in LNG tankers with SPH", *International Conference on Computational Methods in Marine Engineering*, Barcelona, Spain, June.

Fang, Q., Qian, Q.H. and Shi, Y.L. (1996), "A rate-sensitive analysis of R/C beams subjected to blast loads", *International Conference on Structures under Shock and Impact*, Udine, May.

Fu, H.C., Erki, M.A. and Seckin, M. (1991), "Review of effects of loading rate on reinforced concrete", *J. Struct. Eng*., **117**(12), 3660-3679.

Ha, J.H., Yi, N.H., Choi, J.K. and Kim, J.H.J. (2011), "Experimental study on hybrid CFRP-PU strengthening effect on RC panels under blast loading", *Comp. Struct.*, **93**(8), 2070-2082.

Hallquist, J.O., Wainscott, B. and Schweizerhof, K. (1995), "Improved simulation of thin-sheet metalforming using LS-DYNA3D on parallel computers", *J. Mater. Proc. Tech.*, **50**(1), 144-157.

Heo, Y. and Kunnath, S.K. (2013), "Damage-based seismic performance evaluation of reinforced concrete frames", *Int. J. Concrete Struct. Mater.*, **7**(3), 175-182.

Jeon, S.J., Jin, B.M., Yoo, J.W. and Kim, Y.J. (2003), "Design basis for large above-ground LNG tank", *J. Korea Concrete Inst.*, **15**(3), 31-37.

Jiang, H., Wang, X. and He, S. (2012), "Numerical simulation of impact tests on reinforced concrete beams", *Mater. Des.*, **39**, 111-120.

Kim, C.K. and Kim, H.G. (2005), "Optimized design of roof structure in LNG storage tank", *J. Korean Inst. Gas*, **9**(4), 36-43.

Kim, H.J., Nam, J.W., Kim, S.B., Kim, J.H. and Byun, K.J. (2007), "Analytical evaluations of the retrofit performances of concrete wall structures subjected to blast load", *J. Korea Concrete Inst.*, **19**(2), 241-250.

Kim, T.H., Seong, D.J. and Shin, H.M. (2012), "Seismic performance assessment of hollow reinforced concrete and prestressed concrete bridge columns", *Int. J. Concrete Struct. Mater.*, **6**(3), 165-176.

Larcher, M. (2007), "Simulation of the effects of an air blast wave", Luxemburg Office of Official Publications of the European Communities. Luxemburg.

Le Blanc, G., Adoum, M. and Lapoujade, V. (2005), "External blast load on structures–Empirical approach", *5th European LS-Dyna Users Conference*, Paris, May.
Li, J. and Hao, H. (2013), "Influence of brittle shear damage on accuracy of the two-step method in prediction of structural response to blast loads", *Int. J. Impact Eng.*, **54**, 217-231.
Li, Y., Wang, X. and Guo, X. (2006), "Experimental study on anti-impact properties of a partially prestressed concrete beam", *Explos. Shock Waves*, **26**(3), 256.
Lin, X., Zhang, Y.X. and Hazell, P.J. (2014), "Modelling the response of reinforced concrete panels under blast loading", *Mater. Des.*, **56**, 620-628.
LSTC, L.D. (2010), *Version 971 Keyword User's Manual_Rev5-Beta*, Livermore Software Technology Corporation, Livermore, CA, USA.
Luccioni, B.M., Ambrosini, R.D. and Danesi, R.F. (2004), "Analysis of building collapse under blast loads", *Eng. Struct.*, **26**(1), 63-71.
Magnusson, J. and Hallgren, M. (2003), "High performance concrete beams subjected to shock waves from air blast", Swedish Defence Research Agency.
Malvar, L.J. (1998), "Review of static and dynamic properties of steel reinforcing bars", *ACI Mater. J.*, **95**(5), 609-616.
Malvar, L.J. and Ross, C.A. (1998), "Review of strain rate effects for concrete in tension", *ACI Mater. J.*, **95**(6), 735-739.
Ngo, T., Mendis, P. and Krauthammer, T. (2007), "Behavior of ultrahigh-strength prestressed concrete panels subjected to blast loading", *J. Struct. Eng.*, **133**(11), 1582-1590.
Qin, F. and Pingan, W. (2003), "Main factors affecting failure modes of blast loaded RC beams", *Chinese J. Comput. Mech.*, **1**, 009.
Shi, Y., Hao, H. and Li, Z.X. (2008), "Numerical derivation of pressure–impulse diagrams for prediction of RC column damage to blast loads", *Int. J. Impact Eng.*, **35**(11), 1213-1227.
Wang, F., Wan, Y.K.M., Chong, O.Y.K., Lim, C.H. and Lim, E.T.M. (2008), "Reinforced concrete slab subjected to close-in explosion", *Proc., 7th German LS-DYNA Forum*, Bamberg, Germany, September.
Yi, N.H., Kim, J.H.J., Han, T.S., Cho, Y.G. and Lee, J.H. (2012), "Blast-resistant characteristics of ultra-high strength concrete and reactive powder concrete", *Constr. Build. Mater.*, **28**(1), 694-707.